Mon. Not. R. Astron. Soc. **318**, 214–226 (2000)

Exospheric models for the X-ray emission from single Wolf–Rayet stars

R. Ignace,[1★†] L. M. Oskinova[1] and C. Foullon[2]
[1]*Department of Physics and Astronomy, University of Glasgow, Glasgow G12 8QQ*
[2]*Mathematical Institute, University of St Andrews, St Andrews KY16 9SS*

Accepted 2000 May 25. Received 2000 April 26; in original form 2000 February 24

ABSTRACT

We review existing *ROSAT* detections of single Galactic Wolf–Rayet (WR) stars and develop wind models to interpret the X-ray emission. The *ROSAT* data, consisting of bandpass detections from the *ROSAT* All-Sky Survey (RASS) and some pointed observations, exhibit no correlations of the WR X-ray luminosity (L_X) with any star or wind parameters of interest (e.g. bolometric luminosity, mass-loss rate or wind kinetic energy), although the dispersion in the measurements is quite large. The lack of correlation between X-ray luminosity and wind parameters among the WR stars is unlike that of their progenitors, the O stars, which show trends with such parameters. In this paper we seek to (i) test by how much the X-ray properties of the WR stars differ from the O stars and (ii) place limits on the temperature T_X and filling factor f_X of the X-ray-emitting gas in the WR winds. Adopting empirically derived relationships for T_X and f_X from O-star winds, the predicted X-ray emission from WR stars is much smaller than observed with *ROSAT*. Abandoning the T_X relation from O stars, we maximize the cooling from a single-temperature hot gas to derive lower limits for the filling factors in WR winds. Although these filling factors are consistently found to be an order of magnitude greater than those for O stars, we find that the data are consistent (albeit the data are noisy) with a trend of $f_X \propto (\dot{M}/v_\infty)^{-1}$ in WR stars, as is also the case for O stars.

Key words: stars: abundances – stars: early-type – stars: Wolf–Rayet – X-rays: stars.

1 INTRODUCTION

In 1867, Wolf & Rayet discovered three early-type stars with anomalously strong and broad emission bands. Today only about 200 of these hot ($\gtrsim$30 000 K), luminous (absolute magnitudes M_V from -4.5 to -6.5) Wolf–Rayet stars are known in the Galaxy. They are characterized by high masses ($\sim$10–40 $M_\odot$) with strong stellar winds. Helium-rich and hydrogen-deficient, nitrogen is prominent in some, the WN stars, whereas carbon is significant in the spectra of others, the WC stars. There is even a minority class of oxygen-rich WO stars. These unusual compositions suggest that WR stars are evolved phases of massive stars.

The O- and B-star winds are reasonably well described by the radiative line-driven wind theory of Castor, Abbott & Klein (1975, hereafter CAK), but a good understanding of how the dense Wolf–Rayet (WR) winds are driven remains somewhat elusive in spite of recent advances in theory and observations. It is well known that the momentum of WR winds $\dot{M}v_\infty$ typically exceeds the single-scattering limit L_*/c by an order of magnitude (e.g. Willis 1991). There have been numerous attempts to explain the large values of $\dot{M}v_\infty$, for example, considerations of wind clumping (Nugis, Crowther & Willis 1998), non-spherical geometries (Ignace, Cassinelli & Bjorkman 1996), magnetic fields (Poe, Friend & Cassinelli 1989; dos Santos, Jatenco-Pereira & Opher 1993) or super-Eddington winds (Kato & Iben 1992). The most promising model for accelerating the high-mass-loss WR winds derives from multiline scattering of photons (Lucy & Abbott 1993; Springmann 1994; Gayley, Owocki & Cranmer 1995). This theory is indeed fully capable of explaining the driving of WR winds, provided that the opacity is sufficient for photons to be scattered frequently ($\sim$100 times) among different lines. Of especial relevance to this work, Gayley & Owocki (1995) have shown that even with multiple scattering, the instability mechanism that leads to shock formation in the lower mass-loss OB star winds should still operate in the WR winds, and so potentially provide a mechanism for producing the observed X-ray emission.

The first quantitative X-ray information on WR stars was obtained with *Einstein* by Seward & Chlebowski (1982), who detected WR25 (HD 93162). White & Long (1986) obtained observations of WR6 (EZ CMa, HD 50896). Both data sets were fitted with thermal bremsstrahlung models for hot gas around 10^7 K and hydrogen column densities $N_H \sim 10^{22}$ cm^{-2}. Although *Einstein*'s spectral response of 0.2–4 keV had the potential of providing exciting results on WR winds, only WR25 and WR6

★ Present address: 203 Van Allen Hall, Physics and Astronomy, University of Iowa, Iowa City, IA 52242, USA.
† E-mail: ri@astro.physics.uiowa.edu

had sufficient integration time to yield useful spectra. Pollock (1987) has reviewed the passband detection of single and binary WR stars by *Einstein*. He notes that single stars of the WN subclass appear to be about 4 times brighter than single WC stars. He suggests that this might be the result of very different abundances between the two subclasses. Pollock, Haberl & Corcoran (1995) have published a table of PSPC passband detections and upper limits for all Galactic WR stars from the *ROSAT* All Sky Survey (RASS). In terms of *ROSAT* spectra, Wessolowski et al. (1995) obtained nine pointed observations of single WN stars, with enough signal to yield spectra for WR 1 and WR 110.

ASCA has a higher energy response and greater spectral resolution than *ROSAT* or *Einstein*, but has observed only four WR stars: WR6, WR139, WR140 and WR147 (Koyama et al. 1994; Stevens et al. 1996; Skinner, Itoh & Nagase 1997; Maeda et al. 1999). WR6 has an observed stable period of 3.766 d and may be a binary. The other three are definite WR+O binaries, in which wind interactions are important for the X-ray production. Similarly, only WR binaries are to be observed with *Chandra* during its first cycle. However, at least a couple of single WR targets will be observed with *XMM*. Overall, there has been considerable activity in observing colliding wind binary systems with WR components, but relatively little has been done with recent X-ray satellites to study single-star WR envelopes.

None the less, there have been some advances in studies of X-rays from single WR stars. The RASS has provided PSPC broad-band fluxes in the range 0.2–2.4 keV for nearly all Galactic WR stars (Pollock et al. 1995). This data set has revealed that, unlike their predecessors (the O stars), the X-ray luminosities $L_{\rm X}$ of single N-rich WR types (WN) are *not* correlated with bolometric luminosity $L_{\rm Bol}$, wind momentum $\dot{M}v_\infty$, wind kinetic luminosity $\dot{M}v_\infty^2$, or WN subtype (Wessolowski 1996).

On the side of theory, Baum et al. (1992) presented model results for X-ray spectra from single WR stars. The models took account of the non-solar abundances in terms of the attenuation of X-rays by the cool wind; however, the emission is based on purely thermal bremsstrahlung only. It seems likely that cooling via line emission of highly ionized species, as in the Raymond & Smith (1977, hereafter RS) models for hot optically thin plasmas, will be important, especially owing to the highly enhanced metal abundances of WR winds. Ignace & Oskinova (1999, hereafter Paper I) have sought to explain the trends (or rather the lack of trends) found by Wessolowski (1996). The cool dense WR winds are optically thick to X-rays for a broad range of energies, so that observed X-ray emission can be thought as forming exterior to an 'exosphere', a surface defined by optical depth unity in the cool wind opacity. If the filling factor of hot gas (to be discussed below) scales inversely with the ratio $\dot{M}/v_\infty$ (i.e., the wind density scale), all dependence on $\dot{M}/v_\infty$ exactly cancels, and the $L_{\rm X}$ values will show no correlations with such mass-loss, terminal speed, or any combination thereof. Instead, there exists a dependence on abundances, and although the dispersion of the *ROSAT* measurements is relatively large, it was found in Paper I that the differences in abundances between the WC and WN classes may be sufficient to explain why WN winds tend to be about 3–4 times more X-ray-luminous than WC winds (confirming Pollock's 1987 suggestion).

In this paper the analysis is taken one step further in an attempt to assess the hot gas temperatures and filling factors. In Section 2 we expand on the emission model used in Paper I. We especially elaborate on the effects of abundances for the wind attenuation. In Section 3 we apply these models in several different ways, the chief aim being to set limits on the hot gas filling factor and to test the hypothesis that these filling factors vary inversely with the ratio $\dot{M}/v_\infty$. A discussion of these results is presented in Section 4. Appendices detail some of the more technical aspects of the emission modelling, and also the linear regression scheme in fitting the data and model results.

2 SPECIFICATION OF THE MODEL

We consider a spherically symmetric and time-independent stellar wind that is a homogeneous mix of 'cool' and 'hot' gas in dynamical equilibrium. The ambient stellar wind consists predominantly of the cool gas component ($\lesssim 10^5$ K), whereas the minor hot gas component ($\gtrsim 10^6$ K) gives rise to the X-ray emission. This hot gas emission is modelled as an optically thin hot plasma that is characterized by a 'filling factor', defined so that the emitted power in X-rays from a differential volume element dV is

$$\mathrm{d}L_{\rm X}(E) = 4\pi j_\nu \,\mathrm{d}V = f_{\rm X} n_{\rm e} n_{\rm i} \Lambda_\nu(T_{\rm X})\,\mathrm{d}V, \tag{1}$$

where j_ν is the emissivity, $f_{\rm X}$ is the filling factor, $n_{\rm e}$ and $n_{\rm i}$ are the electron and ion densities of the cool or normal wind component, Λ_ν is the cooling function, and $T_{\rm X}$ is the temperature of the hot gas. This definition for the filling factor is the same as that used by Kudritzki et al. (1996), so that we may make reference to their results at a later point. Note that, in general, $f_{\rm X}$, $T_{\rm X}$, $n_{\rm e}$ and $n_{\rm i}$ are potentially all functions of radius. However, observations of single WR stars consist mainly of broad-band X-ray fluxes, so that in this paper $f_{\rm X}$ and $T_{\rm X}$ will be treated as constants throughout the wind flow, for simplicity. Without spectral information, there is little to constrain any possible radial dependence of $f_{\rm X}$ and $T_{\rm X}$, if it exists.

The total specific luminosity emerging from the wind is given by a volume integral over the observable envelope:

$$L_{\rm X}(E) = \int_V f_{\rm X} n_{\rm e} n_{\rm i} \Lambda_\nu(T_{\rm X}) e^{-\tau_{\rm w}}\,\mathrm{d}V, \tag{2}$$

where $\tau_{\rm w}$ is the attenuation of X-rays by the wind. Self-absorption by the hot plasma is ignored. The attenuation is therefore entirely from the cool wind component intervening between the observer and the point of emission. The wind optical depth is given by

$$\tau_{\rm w}(p,z) = \int_z^\infty \kappa_{\rm w}\rho\,\mathrm{d}z, \tag{3}$$

with opacity $\kappa_{\rm w}$ and density

$$\rho(r) = \frac{\dot{M}}{4\pi r^2 v_{\rm r}(r)}. \tag{4}$$

For the radial wind speed, it is standard to assume a β velocity with

$$v_{\rm r}(r) = v_\infty\left(1 - \frac{bR}{r}\right)^\beta, \tag{5}$$

where the non-dimensional constant $b < 1$, and R is the radius at the wind base (taken to be the radius of the star). Including the parameter b ensures that the density is not singular at the lower boundary. However, in our analysis it will be sufficient to assume that the X-rays emerge from large radius only, where $v_{\rm r}(r) \approx v_\infty$.

The dominant opacity at the X-ray energies is photo-absorption by K-shell electrons. This opacity is

$$\kappa_{\rm w}(E) = \frac{1}{\mu_{\rm N} m_{\rm H}} \sum_j \frac{n_j}{n_{\rm N}}\,\sigma_j(E). \tag{6}$$

The opacity is a summation over cross-sections σ_j presented by different atomic species j and weighted by the relative abundance n_j/n_N, for n_N the number density of nuclei. The factor of μ_N is the mean molecular weight per nucleus, but since there is essentially no neutral gas in hot-star winds, the number density of nuclei is the same as ions; hence $n_N = n_i$ and $\mu_N = \mu_i$.

Abundances can have an important effect on the emergent X-ray luminosity, both in terms of the cool wind attenuation and the emissivity. With the above expressions constituting our basic model for the X-ray emission from hot-star winds, we now address the consequences of the highly non-solar abundances of the WR stars for the various factors that determine the X-ray luminosity.

Table 1. Wolf–Rayet abundances (by number).

Element	Cosmic	WN	WC
H	0.922	0.0625	0.0
He	0.0766	0.93	0.618
C	3.67e−4	1.19e−3	0.248
N	1.03e−4	5.85e−3	0.0
O	8.21e−4	2.72e−4	0.12
Ne	9.2e−5	6.11e−4	0.0115
Mg	2.3e−5	2.04e−4	1.68e−3
Si	2.9e−5	2.01e−4	4.23e−4
P	–	9.83e−7	1.95e−6
S	2.07e−5	4.75e−5	9.4e−5
Fe	5.5e−5	1.19e−4	2.36e−4

2.1 The effect of abundances for the wind opacity

For the wind attenuation of the X-rays, K-shell absorption by metals in the cool wind is the dominant opacity source. The contribution to the absorptive opacity can vary strongly with atomic species, as for example in the case of H-like atoms where the cross-section scales as the fourth power of the proton number. So even modest enhancements of metals from nuclear burning can dramatically alter the run of wind opacity with wavelength. Table 1 contrasts typical abundances of WN and WC stars (taken from van der Hucht, Cassinelli & Williams 1986) against cosmic abundances. The WN types are essentially helium stars with enhanced nitrogen and an underabundance of oxygen. The WC stars are essentially helium-carbon stars with substantial amounts of oxygen but essentially no nitrogen.

Fig. 1 displays the energy-dependent photoelectric cross-sections $\sigma_w(E) = \mu_N m_H \kappa_w$ in units of cm^2 per particle for stars of different metallicities and ionization states of hydrogen and helium. The curves were computed using codes made available by Balucińska-Church & McCammon (1992) that allow the abundances to be

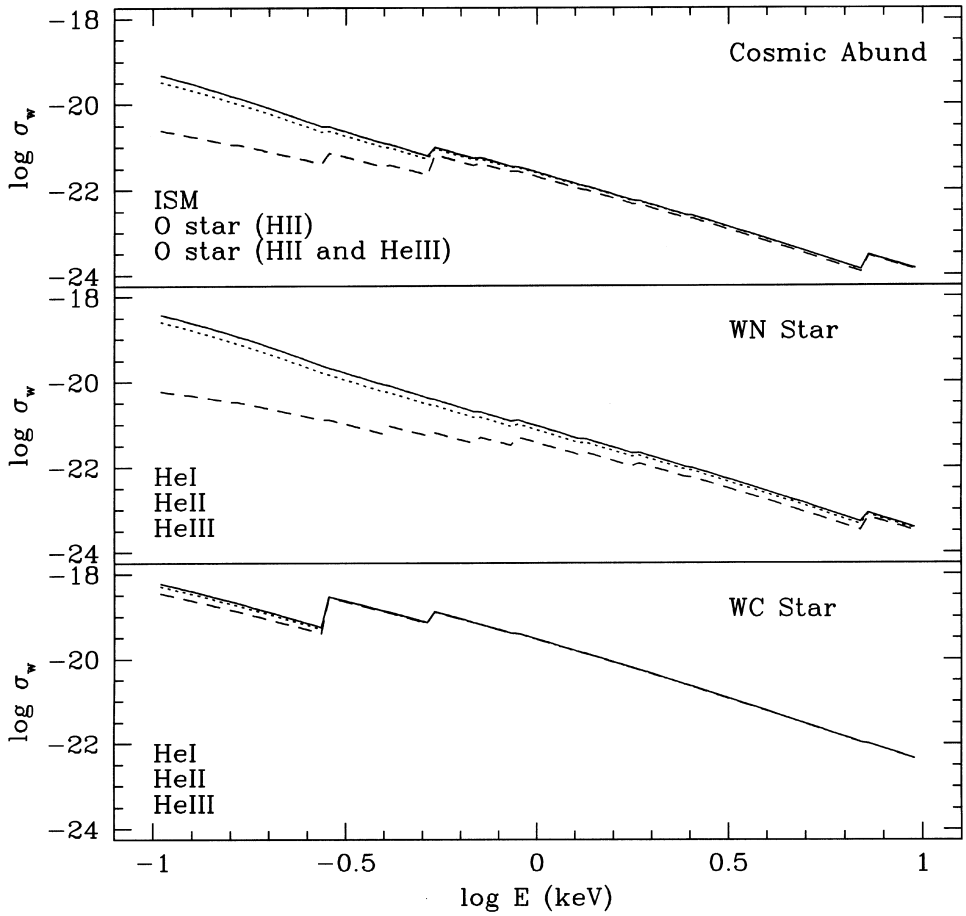

Figure 1. Shown are plots of the absorption cross-section σ_w in cm^2 of the cool wind to X-rays as a function of energy. The top, middle, and bottom panels are for cosmic, WN, and WC abundances. For the purposes of this work, it is adequate to treat O stars as having cosmic abundances. In the top panel, the solid line is for a gas with H I, like the ISM, the dotted line is for an O star with H II, and the dashed line is for an O star with H II and He III. For both the WN and WC cases, hydrogen is assumed ionized or absent altogether. Solid, dotted, and dashed lines are then for neutral, once-ionized, and twice-ionized helium. In our models we always take helium to be once-ionized in the WR winds.

input parameters. Prominent edges can be seen at 0.28, 0.40 and 0.53 keV for the C, N and O atoms. Note that the Balucińska-Church & McCammon opacities are for neutral species. They comment that ionization of metals does not much affect the magnitude of the absorption cross-section, but it does shift the edge energy. Tabulations by Verner & Yakovlev (1995) indicate that the edge energy moves to increasingly large values for more highly ionized species. The change in edge energy between any two ions is just a few per cent, but the jump from a neutral atom to a hydrogenic atom is around 50 per cent or more (e.g., the edge for O I is 0.53 keV, but that for O VIII is 0.87 keV). An element that is entirely ionized obviously makes no contribution to σ_w, which is relevant for hydrogen and possibly helium in the cool component gas of early-type winds. In our models we use edges for neutral metals.

In Fig. 1 the top panel shows three curves: solid for the standard cross-section appropriate to the ISM with cosmic abundances, dotted for an O star with cosmic abundances and completely ionized hydrogen, and dashed for the same O star but with helium completely ionized. The drop in the cross-section at low energies is similar to that found by Hillier et al. (1993) in their study of ζ Puppis (O4f) which included the effects of helium ionization. The middle panel is for a hydrogen-deficient WN star, with a solid curve for He I, a dotted one for He II, and a dashed one for He III. Comparing the solid curves for an O and WN star, the cross-section for the latter is higher by about 0.5 dex at high energies and 0.8 dex at lower energies. Note, however, that $\mu_i(\mathrm{WN}) \approx 3\mu_i(\mathrm{O})$, so that the opacity κ_w is nearly the same for both O and WN stars. The greater attenuation of X-rays in WN winds relative to O stars is mostly a consequence of higher wind density.

The bottom panel of Fig. 1 is for a WC star with different ionizations of helium. The curves are relatively insensitive to helium ionization. The carbon edge is extremely prominent, and the overall cross-section is up by about 1.5 dex near 1 keV over that for a WN star (but this increment clearly varies strongly with energy). The ion mean molecular weight is greater in WC stars, being about 2 times that for WN stars and 6 times that for O stars, so in this case the opacity is actually significantly larger in WC stars than in other hot stars with less enhanced abundances.

2.2 The effect of abundances for the cooling function

For temperatures T_X in which Λ_ν is dominated by line emission (in contrast to thermal bremsstrahlung that dominates for $T_X \gtrsim 10^8$ K), the cooling function is roughly given by $\Lambda_\nu \approx \sum_k P_k n_k/n_i$, where P_k is a factor relating to the emitted power in the line k and will generally depend on density and temperature, and n_k/n_i is the ratio of the number density population corresponding to the line k to the total ion number density of the hot gas. For solar abundances, the RS cooling function is used, with $\Lambda_{RS} \approx \sum_k P_k(T)(n_k/n_H)_\odot$, where n_H is the ionized hydrogen density of the hot gas. Assuming that the P_ks vary weakly with density and temperature, and further that the ratio $n_k/(n_k)_\odot = \tilde{\mathcal{A}}$ is constant for every line k, a scaling correction to the known RS cooling function for non-solar abundances is (see Appendix A)

$$\Lambda_\nu(T_X) \approx \frac{\mu_i}{\mu_{H,\odot}}\,\tilde{\mathcal{A}}\Lambda_{RS}(E,T_X), \tag{7}$$

where $\mu_{H,\odot}$ is the mean molecular weight per ionized hydrogen atom for solar abundances, which is the same for both the cool and the hot gas. In the case that $n_k/(n_k)_\odot$ is not constant for every k, $\tilde{\mathcal{A}}$ is an overall average enhancement (or reduction) factor to the RS cooling function. This latter interpretation of $\tilde{\mathcal{A}}$ is the most relevant to our case, since the *ROSAT* data that we will consider consists of bandpass fluxes, wherein the contributions of many lines are being summed together.

In Paper I we used an ion mean molecular weight for WN stars of $\mu_i = 4$ and for WC stars $\mu_i = 7.6$. We also argued for $\tilde{A}_{WN} \approx 1$, because the evolution from O stars to WN stars mostly results in converting hydrogen to helium, some enhancement of nitrogen, and a depletion of oxygen, elements that have relatively little consequence for the cooling function. On the other hand, further evolution to WC stars leads to substantial enhancements of carbon and oxygen, essentially the elimination of nitrogen, but also enhancements in neon and magnesium – changes with greater relevance for the relative intensity of some lines that appear at *ROSAT* energies. In this case $\tilde{A}_{WC} \geq 1$ is likely, with values of perhaps a few. For example, Koyama et al. (1994) require the abundance of neon to be about 100 times solar to explain the *ASCA* spectrum WR 140 (WC + O4–5). The enhanced neon is surely not from the O-star companion. The spectral feature they fit is at about 1.2 keV, which falls midway in the *ROSAT* band, so there is good reason to believe that $\tilde{A}_{WC}$ could be a few or greater. Taking $\mu_{H,\odot} \approx 1.5$, we estimate that $\Lambda_\nu/\Lambda_{RS} \approx 3$ for WN stars, and at least that for WC stars.

2.3 The effect of abundances for the filling factor

We assume the filling factor to be constant throughout the wind, with a value that can vary between different stars. First, it can vary with abundance as $f_X \propto (\mu_e\mu_i)_w/(\mu_e\mu_i)_X = (\mu_e)_w/(\mu_e)_X$. Note that $(\mu_e)_w/(\mu_e)_X \lesssim 2$ for reasonable assumptions about the ionization state in the cool and hot components, so this does not provide much variation in f_X among different stars. The filling factor is also taken to vary inversely with the ratio $\dot{M}/v_\infty$. For example, Kudritzki et al. (1996) has analysed *ROSAT* observations for 42 O stars, and empirically determined $f_X \propto (\dot{M}/v_\infty)^{-1}$. They attribute this result to the expectation that larger ratios of $\dot{M}/v_\infty$ result in more efficient cooling, shorter cooling zones, and consequently smaller filling factors (see also discussion by Hillier et al. 1993). The end result is that the volume filling factor scales as

$$f_X \propto \frac{(\mu_e)_w}{(\mu_e)_X}\left(\frac{\dot{M}}{v_\infty}\right)^{-1}. \tag{8}$$

Note that in the context of explaining the X-ray emission from O stars, Owocki & Cohen (1999) consider a filling factor that varies with radius as a power law. However, they do not consider how f_X might vary from star to star. They are able to explain the observed relation between L_X and L_{Bol} (which they identify as really being related to $\dot{M}/v_\infty$) by adjusting the power-law exponent for the filling factor. Owing to the poorer data for single WR stars (no spectra and fairly large errors for bandpass measurements), it was assumed in Paper I that the filling factor of equation (8) is constant in the flow, but could vary from wind to wind. In Paper I the lack of correlations between L_X and wind parameters could then be explained. However, if f_X is not constant in the wind, an analysis like that of Owocki & Cohen will be needed to explain the observed lack of correlation. So the conclusion of Paper I is clearly model-dependent, but the assumptions adopted in Paper I do appear to be sufficient to explain the data.

2.4 The exospheric approximation

In their study of X-rays from OB stars, Owocki & Cohen (1999) presented a scaling analysis for the X-ray emission from hot-star winds based on an exospheric approximation. The observed X-ray emission arising from hot gas emerges only from radii exterior to the optical depth unity surface of radius r_1, with X-rays at smaller radii assumed to be completely attenuated. The extent of r_1 is energy-dependent, with

$$r_1(E) = \frac{\dot{M}}{4\pi v_\infty}\kappa_{\rm w}(E). \tag{9}$$

Owocki & Cohen showed that for a constant expansion wind, the exospheric approximation overestimates $L_{\rm X}$ from an exact integration for the radiative transfer by a factor of only 2. Since $r_1 \gg R_*$ over a broad range of X-ray energies for the WR stars, a constant expansion wind is an excellent approximation. For the purposes of modelling the X-rays, we therefore assume a spherical wind with density $\rho = \dot{M}/4\pi v_\infty r^2$ for WR stars.

The emergent specific X-ray luminosity (including a factor of 2 reduction for the reasons just discussed) is thus given by

$$L_{\rm X}(E) \approx 4\pi^2 \int_{r_1}^{\infty} j_\nu \left(1 + \sqrt{1 - \frac{r_1^2}{r^2}}\right) r^2\, {\rm d}r, \tag{10}$$

where the parenthetical term accounts for geometric occultation by the spherical surface of radius r_1 (a minor 10 per cent effect that was ignored by Owocki & Cohen but which we choose to include). Substituting for the emissivity j_ν,

$$L_{\rm X}(E) = \frac{1+\pi/4}{16\pi}\frac{\dot{M}^2}{\mu_{\rm e}\mu_{\rm i} m_{\rm H}^2 v_\infty^2 r_1} f_{\rm X}\Lambda_\nu(T_{\rm X}). \tag{11}$$

Equations (10) and (11) are the same as those used in Paper I. Substituting for the factor r_1 yields

$$L_{\rm X}(E) = \frac{1+\pi/4}{4}\frac{\dot{M}}{\mu_{\rm e}\mu_{\rm i} m_{\rm H}^2 v_\infty \kappa_{\rm w}(E)} f_{\rm X}\Lambda_\nu(T_{\rm X}). \tag{12}$$

The energy dependence of $L_{\rm X}(E)$ comes strictly from the ratio

Table 2. Wolf–Rayet X-ray and wind parameters for WN stars.

WR #	$\log L_{\rm X}/{\rm L}_\odot$	$\sigma(\log L_{\rm X}/{\rm L}_\odot)$	$\log L_*/{\rm L}_\odot$	$\log \dot{M}$ ($M_\odot\,{\rm yr}^{-1}$)	v_∞ (km s^{-1})	T_* (kK)	R_* ($R_\odot$)	M_* ($M_\odot$)	$E(b-v)$	D (kpc)	Subtype
1	−0.63	0.01	5.3	−4.1	2000	100.0	1.5	13	0.59	2.6	WNE
2	−1.63	0.07	5.0	−4.5	3100	141.3	0.5	9	0.49	2.5	WNE
3	−1.67	0.31	5.6	−5.1	2500	89.1	2.5	18	0.33	3.0	WNE
6	−0.87	0.03	5.4	−4.1	1700	100.0	1.8	16	0.03	1.8	WNE
7	−1.20	0.15	5.3	−4.4	1600	89.1	1.9	13	0.46	5.8	WNE
10	−1.19	0.23	5.9	−5.0	1500	63.1	7.5	28	0.60	4.6	WNE
12	−0.09	0.23	5.8	−3.6	1100	35.5	19.9	23	0.65	11.0	WNL
16	−1.16	0.28	5.8	−3.8	900	31.6	25.1	23	0.50	4.4	WNL
18	−1.22	0.14	5.7	−4.0	2100	100.0	2.4	22	0.64	4.6	WNE
22	−1.12	0.26	6.0	−4.4	1000	35.5	26.5	33	0.31	2.6	WNL
24	−1.54	0.33	5.9	−4.5	1200	35.5	23.6	28	0.26	2.6	WNL
25	0.10	0.008	5.4	−4.9	1200	35.5	13.3	15	0.40	2.6	WNL
34	0.18	0.43	5.4	−4.5	1200	63.1	4.5	16	0.97	9.1	WNE
35	−0.11	0.43	5.4	−4.3	1100	39.8	11.2	16	1.01	11.0	WNE
36	−0.84	0.43	5.3	−4.2	2100	89.1	2.0	14	0.95	5.2	WNE
37	−1.02	0.43	5.1	−4.6	2150	79.4	1.9	10	1.70	2.6	WNE
44	−0.94	0.46	5.6	−4.9	1400	70.8	4.0	18	0.61	7.6	WNE
46	−1.34	0.15	5.4	−4.9	2300	89.1	2.2	16	0.0	3.2	WNE
49	−0.37	0.26	5.7	−4.7	1450	70.8	4.7	22	0.9	7.9	WNE
51	−0.32	0.36	5.5	−4.8	1300	63.1	4.7	17	1.45	3.6	WNE
54	−0.89	0.23	5.5	−4.8	1300	70.8	3.7	17	0.8	5.2	WNE
62	−1.28	0.27	5.4	−3.8	1800	44.7	8.9	16	1.9	2.4	WNE
66	−0.37	0.21	5.8	−3.6	1500	31.6	25.1	23	1.0	7.9	WNL
67	−0.54	0.23	5.1	−4.4	1500	39.8	7.5	10	0.97	3.6	WNE
74	−0.58	0.22	5.9	−3.7	1300	39.8	18.8	28	1.9	4.0	WNL
75	−0.50	0.18	5.8	−3.7	2300	56.2	8.4	25	1.0	4.0	WNE
82	−0.35	0.43	5.9	−3.8	1100	39.8	19.9	31	1.07	9.5	WNL
84	−0.26	0.93	5.5	−4.2	1100	39.8	11.9	17	1.50	3.8	WNE
89	−0.68	0.28	6.3	−4.1	1600	35.5	35.4	47	1.65	2.9	WNL
100	−0.77	0.24	5.3	−3.7	1600	44.6	7.9	14	1.4	4.4	WNE
105	−1.31	0.34	5.8	−4.2	700	31.6	26.6	25	2.13	1.6	WNL
108	−0.96	0.24	5.8	−4.6	900	31.6	26.6	25	1.01	3.5	WNL
110	−0.71	0.04	5.9	−3.7	2300	89.1	4.0	30	0.90	2.6	WNE
115	−1.50	0.23	5.6	−4.3	1280	39.8	12.6	18	1.50	2.2	WNE
116	−0.93	0.26	5.8	−3.7	800	31.6	25.1	23	1.69	2.6	WNL
120	−0.85	0.28	5.9	−3.8	1020	35.5	23.6	28	1.35	5.2	WNL
123	−0.55	0.35	5.7	−3.7	1020	31.6	23.7	22	0.71	11.0	WNL
128	−1.83	0.65	5.5	−5.2	1500	63.1	4.7	17	0.32	4.2	WNE
134	−1.93	0.21	6.0	−3.9	1900	89.1	4.2	33	0.47	2.1	WNE
136	−2.31	0.18	6.1	−3.9	1600	70.8	7.5	38	0.5	1.8	WNE
148	−1.14	0.23	6.0	−4.5	1000	35.5	26.5	30	0.90	5.2	WNL
149	−0.49	0.27	5.7	−4.1	1100	50.1	9.4	22	1.50	9.5	WNE
152	−1.71	0.25	5.4	−5.2	1800	79.4	2.7	22	0.5	3.5	WNE
157	−1.22	0.22	5.9	−4.4	1500	39.8	19.9	30	0.85	3.6	WNE
158	−0.65	0.20	5.9	−4.3	900	35.5	23.6	28	1.05	6.3	WNL

$\Lambda_\nu/\kappa_w(E)$. Also, note that $L_X(E)$ appears to scale with the ratio $\dot{M}/v_\infty$; however, the hot gas filling factor f_X implicitly depends on $(\dot{M}/v_\infty)^{-1}$. Hence the scaling of X-ray luminosity should not scale with wind mass-loss or terminal speed. Although perhaps T_X may depend on these parameters in some way, it is not clear how this might affect $L_X(E)$. Ignoring any such dependence between T_X and $\dot{M}$ or v_∞, the above expressions were used in Paper I to conclude that X-ray luminosities from WR winds will depend only on abundances.

3 APPLICATION TO THE *ROSAT* DATA

3.1 Description of the data and analysis

Having developed a model for the X-ray emission from WR winds, we now consider the existing *ROSAT* data. Although single and binary WR stars have been observed with several X-ray telescopes, the most 'complete' data set at present comes from the *ROSAT* All-Sky Survey. We have selected single WN and WC stars from the compilation of Pollock et al. (1995). We combine those *ROSAT* passband measurements with wind parameters derived by Hamann & Koesterke (1998) for WN stars and Koesterke & Hamann (1995) for WC stars. The merged data set is shown in Table 2 for WNs and Table 3 for WCs. Note that we have rescaled the X-ray luminosities according to distances from Hamann & Koesterke and Koesterke & Hamann versus those listed by Pollock et al. (1995) to obtain a more consistent data set, as was done by Wessolowski (1996). However, we have attempted no assessment of the distance estimates or corrections to the X-ray fluxes due to interstellar attenuation. We have simply taken these values from the literature, and so it should be borne in mind that errors in those values could affect our conclusions. Also, as noted by Wessolowski, we revise the count rate for WR 25 from 1960 to $194\,\mathrm{k\,s^{-1}}$ owing to a mistaken entry (presumably the standard deviation decreases by a factor of $\sqrt{10}$, although this is not stated).

In Table 4 we list single stars that are neglected in our analysis:

Table 3. Wolf–Rayet X-ray and wind parameters for WC stars.

WR #	$\log L_X/L_\odot$	$\sigma(\log L_X/L_\odot)$	$\log L_*/L_\odot$	$\log \dot{M}$ ($M_\odot\,yr^{-1}$)	v_∞ ($km\,s^{-1}$)	T_* (kK)	R_* ($R_\odot$)	M_* ($M_\odot$)	$E(b-v)$	D (kpc)	Subtype
4	−2.21	0.76	5.00	−4.20	1900	74.10	1.80	–	0.47	2.9	WCE
5	−2.47	1.27	5.10	−4.30	1600	93.30	1.40	–	0.75	2.1	WCE
13	−0.38	0.17	5.10	−4.30	1700	97.70	1.20	–	1.14	3.8	WCE
14	−1.68	0.18	4.90	−4.20	1800	85.90	1.30	–	0.42	2.0	WCE
17	−1.34	0.34	5.10	−4.20	1800	97.70	1.20	–	0.31	5.1	WCE
23	−1.46	0.24	4.90	−4.10	2200	79.60	1.50	–	0.31	2.7	WCE
39	−1.66	0.43	5.10	−4.70	3600	49.00	4.70	–	1.49	2.2	WCE
68	−0.67	0.22	5.50	−3.90	2050	95.50	2.00	–	1.36	4.9	WCL
86	−1.86	0.24	5.50	−4.40	2300	47.80	8.00	–	0.75	2.0	WCL
111	−2.51	0.11	5.00	−4.30	2000	62.50	2.70	–	0.25	1.6	WCE
114	−1.17	0.19	4.70	−4.30	1900	63.10	2.00	–	1.18	2.2	WCE
125	−1.09	0.18	5.20	−4.00	2800	48.00	6.00	–	1.49	2.8	WCL
126	−0.91	0.26	5.20	−4.80	2500	59.30	4.00	–	0.85	5.0	WCE
132	−0.83	0.27	5.10	−4.20	2000	95.50	1.30	–	0.97	4.4	WCE
135	−2.74	0.68	5.30	−4.10	1300	75.90	2.60	–	0.35	2.1	WCL
143	−2.36	0.23	5.00	−4.50	3200	50.70	4.30	–	1.48	0.8	WCE
154	−1.39	0.25	4.90	−4.20	2050	70.80	1.90	–	0.63	3.4	WCE

Table 4. Sources excluded from analysis.

WR #	Subtype	$L_X/L_\odot$	$\sigma(L_X)/L_\odot$	Comment
28	WN	1.28	0.67	Not analysed in Hamann & Koesterke (1998)
63	WN	0.049	0.036	Not analysed in Hamann & Koesterke (1998)
71	WN	0.052	0.043	Not analysed in Hamann & Koesterke (1998)
91	WN	–	–	No conversion to L_X in Pollock et al. (1995)
94	WN	0.046	0.085	Not analysed in Hamann & Koesterke (1998)
109	WN	–	–	No conversion to L_X in Pollock et al. (1995)
129	WN	0.0098	0.084	$\sigma(L_X)/L_X \approx 9$
155	WN	0.0013	0.025	$\sigma(L_X)/L_X \approx 19$
20	WN	<2.03	0.68	3σ upper limit
29	WN	<0.63	0.21	3σ upper limit
40	WN	<0.043	0.014	3σ upper limit
55	WN	<0.92	0.31	3σ upper limit
58	WN	<0.18	0.060	3σ upper limit
61	WN	<0.95	0.32	3σ upper limit
78	WN	<0.021	0.0070	3σ upper limit
87	WN	<0.17	0.056	3σ upper limit
107	WN	<1.45	0.48	3σ upper limit
124	WN	<0.23	0.078	3σ upper limit
33	WC		0.074	3σ upper limit
52	WC	<0.071	0.024	3σ upper limit
150	WC	<0.14	0.047	3σ upper limit

(a) stars that have only upper limits and are therefore neglected in our analysis, (b) stars that have count rates listed in Pollock et al. (1995) but no conversion to L_X, (c) stars that have extremely poor detections with $\sigma/L_X \gtrsim 10$, which we treat as upper limits, and (d) stars that have values of L_X given by Pollock et al. but no corresponding information for $\dot{M}$, etc. by Hamann & Koesterke or Koesterke & Hamann. In this last case, we do use the L_X values in computing mean WN and WC X-ray luminosities, but not in ensemble analyses that require knowledge of wind parameters.

Most of the data have 1σ or better detections, but we do use some with poorer detections. In the case of multiple detections, we take a straight average, but we give preference to pointed observations if the survey result is substantially worse. Our sample is supposed to be of single stars; however, some targets classified as 'abs' systems (showing absorption features but not confirmed binaries) or single-lined spectroscopic binaries are included. It should be borne in mind that the sample is probably not free from binary contamination. Also, WR 25 is included, which has anomalously high X-ray flux and is a suspected binary, although attempts to find a companion have all been negative. We note that the detection rate among both WN and WC stars is around 80–85 per cent (see Table 5).

Table 5. Summary of *ROSAT* detections.

	$\langle L_X\rangle/L_\odot$	$\sigma_X(\langle L_X\rangle)/L_\odot$	Fraction
WN stars (detections)	0.11	±0.018	52/64
WN stars (3σ upper limits[a])	0.55	–	12/64
WC stars (detections)	0.038	±0.013	17/20
WC stars (3σ upper limits)	0.14	–	3/20

[a] We include WR129 and WR155 among the upper limits (see Table 4).

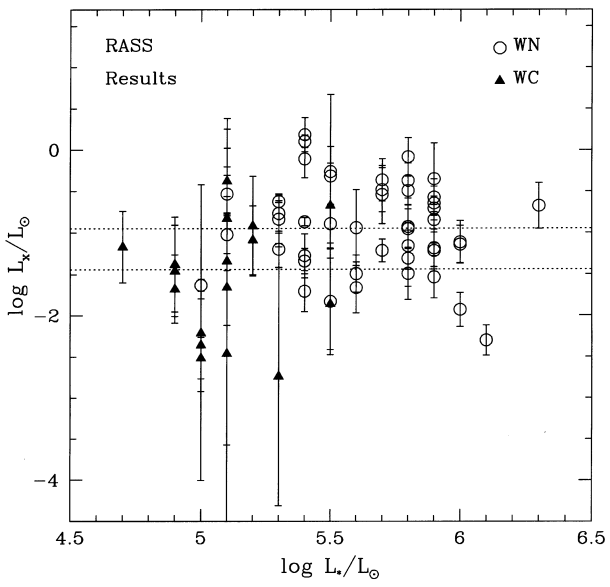

Figure 2. Plot of X-ray luminosity versus bolometric luminosity for *single* WN (circles) and WC (triangles) stars from the RASS and pointed observations. Bolometric luminosities L_* are taken from Koesterke & Hamann (1995) for WC stars and Hamann & Koesterke (1998) for WN stars. The regular spacing in L_* is a reflection of the model gridding in those papers. The measurement errors and dispersion in the points are both substantial, yet there does not appear to be any systematic trend, as is the case for O stars. The two dotted lines are for the weighted mean X-ray luminosities of WN (upper) and WC (lower) stars.

Fig. 2 summarizes this data set as a plot of L_X versus L_* for single WN (circles) and WC (triangles) stars. This is the same figure as that shown in Paper I, except that the errorbars shown in that figure were not properly transformed and have been corrected here. The upper and lower horizontal lines indicate the weighted mean values for the WN subclass and WC subclass respectively. There is substantial scatter in the distribution of X-ray luminosities. Yet there appears to be no linear trend between L_X and L_* as is the case with O stars, neither for the whole ensemble nor for subsets of just the WN stars or just the WC stars. The only overall trend is that WN stars are about 3 times brighter than WC stars in the *ROSAT* band (Paper I and also Table 5), but even this is only a 1σ result.

We have considered a variety of weighted linear regressions to the data sample for L_X versus L_* and $\dot{M}/v_\infty$. The method is described in Appendix B, and a summary of the fits appear in Table 6. The weight for a single measurement i is given by $w_i = 1/(\sigma_i^2 + \sigma_0^2)$, where σ_i is the measurement error, and σ_0 represents an additional dispersion present in the data. This additional spread is motivated by two facts. (a) A standard set of abundances are assumed for the WN types and the WC types, but of course the abundances of any given star will not exactly match the typical values. Variation in abundances among the WN and WC types respectively affects the emergent X-ray emission and introduces an additional dispersion in the data. (b) Likewise, the hot gas temperature is not known and may vary between stars. In all likelihood, it is not even isothermal, with each wind probably showing a range of temperatures in the hot component (e.g., as discussed by Feldmeier et al. 1997). This too introduces additional scatter into the sample. The data are of too poor quality, the spectral information too little (basically none), and abundances not sufficiently well known to account for these variations in each individual star. We therefore seek to account for the variations in a statistical manner through σ_0.

In practice, the most likely value of σ_0 comes from demanding that the reduced chi-square χ^2_ν be unity, where the number of degrees of freedom $\nu = N - 2$ for N data points and a two-parameter line fit. This means that σ_0 is adjusted until the weighted dispersion of the data yields the most probable fit by a straight line. The essential effect of σ_0 is to reduce the importance of those measurements with extremely good measurement errors in the fitting procedure. Again, this is motivated by the a priori realization that the poorly determined abundances and hot gas temperatures introduce an associated dispersion in the data that is unrelated to measurement errors. Only by allowing for this spread can we make a meaningful estimate of mean values or line fits.

The regressions allow for just the WN stars or just the WC stars, or the combined groups. For the WN stars, we show the fit parameters when WR 25 is included or not included, because of its uncertain nature. The case of the filling factors will be discussed later. For L_X versus L_*, there seems to be no hint of a statistically significant linear relation; however, there is a suggestion that perhaps L_X varies with $\dot{M}/v_\infty$ with a power-law index of about 0.3–0.35.

How does one analyse such a data set, and exactly what are the goals of such an analysis, namely what physical parameters are to be constrained? In the context of our model, the fundamental properties relating the observed X-ray emission to the physics of the wind X-ray production are the filling factor, hot gas temperature, and abundances, with everything else taken as known. However, abundances are also not well-known for individual objects, so we will use typical values from Table 1 for all WN and WC stars. The desired result is then to empirically determine f_X

Table 6. Results from linear regression analysis.

Relation	χ^2_ν	m	$\sigma(m)$	b	$\sigma(b)$	σ_0
$\log L_X/L_\odot$ vs $\log L_{Bol}/L_\odot$:	(WN only)					
with WR25	1.0	−0.24	0.28	0.44	1.60	0.50
no WR25	1.0	−0.17	−0.28	−0.02	1.56	0.48
	(WC only)					
	1.0	0.39	0.81	−3.46	4.15	0.625
	(WN and WC)					
WR25	1.0	0.33	0.21	−2.86	1.18	0.555
$\log L_X/L_\odot$ vs $\log \dot{M}/v_\infty$:	(WN only)					
with WR25	1.0	0.26	0.17	1.00	1.23	0.49
no WR25	1.0	0.34	0.16	1.55	1.18	0.45
	(WC only)					
	1.0	0.33	0.65	1.03	4.93	0.625
	(WN and WC)					
with WR25	1.0	0.35	0.17	1.53	1.27	0.545
$\log f_X$ vs $\log \dot{M}/v_\infty$:	(WN and WC)					
with WR25	27.0	−1.13	0.27	−10.80	1.98	0
	1.0	−0.90	0.21	−9.17	1.55	0.69
	0.0	−0.88	0.20	−9.00	1.50	35
no WR25	19.9	−0.68	0.25	−7.47	1.84	0
	1.0	−0.83	0.20	−8.61	1.50	0.655
	0.0	−0.81	0.19	−8.52	1.45	35
	(WN only)					
with WR25	1.0	−0.87	0.20	−9.08	1.47	0.605
no WR25	1.0	−0.76	0.18	−8.28	1.33	0.53
	(WC only)					
	1.0	−0.12	0.72	−2.68	5.50	0.72

and T_X that allow us to affirm, refine, or reject models for the wind driving and/or models for wind structure that leads to the existence of the X-ray-emitting gas.

Given the rather noisy character of the data set, we have selected two different approaches to study the data that each depend on ensemble properties in contrast to tailored fits to individual objects.

(i) First, the winds of O stars are for the most part successfully explained by CAK line-driven wind theory for non-overlapping lines. Lucy & Abbott (1993) find that multiple-scattering effects are probably important for driving the WR winds. Kudritzki et al. (1996) have determined empirical relationships for T_X and f_X based on the wind mass-loss rate and terminal speed. An immediate question is whether the X-ray properties of the WR winds are derivable from the empirical relations that seem to hold for O stars (modulo the effects of highly non-solar abundances for the cooling function and wind attenuation).

(ii) A different approach is to use the data set to place limits on the X-ray temperature or filling factor. We derive a lower limit to the filling factor by maximizing the X-ray emissivity (i.e., for isothermal shocks). This is accomplished by combining the cooling function, *ROSAT* responsivity, and typical wind attenuation dependence with energy to search for a temperature that maximizes the X-ray luminosity sampled in the *ROSAT* bandpass. Assuming this simple temperature to characterize the hot gas in and throughout every WR wind, the filling factor required to explain the observed X-ray emission is thereby minimized in each case.

3.2 Comparison of X-ray properties between O stars and WR stars

Based on figures presented in Kudritzki et al. (1996), we derived the following empirical relations for T_X and f_X for O stars from their figures:

$$T_X^{emp} \approx 10^6\,\mathrm{K}\left(\frac{\dot{M}_{-6}v_{\infty,3}^2}{L_{*,6}}\right)^{0.8}, \tag{13}$$

and

$$f_X^{emp} \approx 2.6\times10^{-3}\left(\frac{\dot{M}_{-6}}{v_{\infty,3}}\right)^{-1.0}, \tag{14}$$

where the numerical subscript stands for powers-of-ten normalization, with $\dot{M}$ in $M_\odot\,yr^{-1}$, v_∞ in $km\,s^{-1}$, and L_* in $L_\odot$. For a typical O star with $\dot{M} = 10^{-6}\,M_\odot\,yr^{-1}$, $T_X^{emp} \approx 4\times10^6$ K or $kT_X^{emp} \approx 0.4$ keV and $f_X^{emp} \approx 7\times10^{-3}$. In contrast, using these relations with typical WR star parameters of $\dot{M} = 3\times10^{-5}\,M_\odot\,yr^{-1}$, $v_\infty = 2000\,km\,s^{-1}$, and $L_* = 3\times10^5\,L_\odot$, the expected hot gas temperature is $T_X^{emp} \approx 10^8$ K and the filling factor $f_X^{emp} \approx 2\times10^{-4}$. If these relations hold for the WR stars, the WR wind should be comparatively much hotter with a far smaller filling factor.

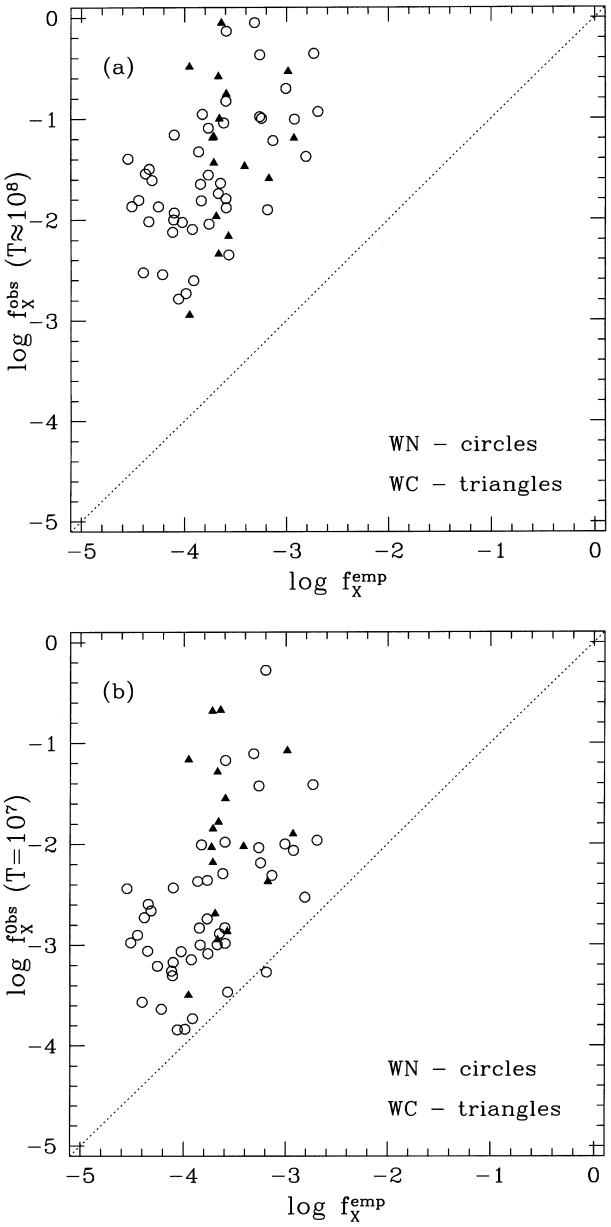

Figure 3. The results of two experiments to compare the inferred filling factors f_X^{obs} of X-ray-emitting gas in WR winds as detected by *ROSAT* against the expected f_X^{emp} values based on an empirical relation derived by Kudritzki et al. (1996) for O stars. WN types are shown as circles, and WC types as triangles. Errorbars are suppressed, but $\sigma \approx 0.3$ is typical. (a) Here the empirical relation for hot gas temperature ($T_X \approx 10^8$ K) was used in computing X-ray emission models from WR winds. (b) A recalculation assuming that all WR stars have $T_X = 10^7$ K. Choosing this temperature maximizes the cooling by lines for the *ROSAT* band (see Fig. 4), so the filling factors are minimized. The ensemble of points drop by about 1 dex, yet still lie systematically above the O-star empirical relation.

To determine whether the O-star relations can be used with WR stars to explain the *ROSAT* observations, we have chosen to assume the Kudritzki et al. (1996) relation for T_X^{emp} as applicable to the WR winds, and then to solve for the filling factor f_X^{obs} required to match the observations. This is accomplished by integrating equation (12) with energy to obtain the predicted X-ray luminosity $L_X^{emp} = L_0 f_X$, where the value of L_0 is based on the energy integration and constants whose values are known or assumed. Setting $L_X^{obs} = L_X^{emp}$, we can solve for the filling factor via $f_X^{obs} = L_X^{obs}/L_0$. In this way the inferred filling factor f_X^{obs} can be compared to that expected from the empirical relation for f_X^{emp}. The results of this experiment are shown in Fig. 3(a). The inferred filling factor is consistently two orders of magnitude *higher* than that expected from the empirical relation.

Although not shown, typical error bars are about 0.3, but can be as high as 1.2. Every star has substantially larger f_X^{obs} than expected from the O-star relation. The high WR filling factors are primarily a result of the high $T_X \sim 10^8$ K as predicted by the empirical relation. At this temperature, the emission is dominantly bremsstrahlung. Although the emission integrated over all energies increases as $T^{1/2}$ for bremsstrahlung, the emission in a fixed energy band decreases as $T^{-1/2}$. Consequently, extremely hot gas in the 10^8 K regime cools much less efficiently at the energies of the *ROSAT* bandpass than does cooler gas of 10^6–10^7 K. So it appears that the physics governing the production of X-rays in the WR winds can not be treated as merely a 'scaled-up' version of what operates in O-star winds.

3.3 Minimal X-ray filling factors for WR winds

In this section we consider the maximum possible emission to determine the minimum filling factor. Results from the previous section suggest that the empirical relations valid for O stars cannot simply be extended to include the WR stars. We make the hypothesis that the temperature relation for O stars almost certainly does not apply. Even in the colliding wind systems of WR binaries, there is little or no evidence for gas at 10^8 K. Such hot gas may be present in small amounts, but the bulk of the X-rays appear to come from lower temperature ($10–30\times10^6$ K) gas. It seems unlikely then that single WR stars would have 10^8 K gas.

On the other hand, the filling factor scales roughly as the inverse of the density. That is a somewhat more robust expectation, namely that cooling is more efficient for higher density material. This would appear to be insensitive to the details of the wind driving or shock formation mechanism(s). Perhaps the temperature relation of Kudritzki et al. (1996) fails miserably when applied to WR stars, but the filling factor scaling $f_X \propto (\dot{M}/v_\infty)^{-1}$ may still be valid, an assumption that was made in the analysis of Paper I and which we seek to show a posteriori.

So, to set a lower limit on the filling factor, it is important to maximize the cooling function not in an absolute sense, but rather with respect to what *ROSAT* can detect. Fig. 4 summarizes the steps in doing this. The open boxes connected by the short-dashed curve plot the spectrum-integrated RS cooling function against temperature T_X. Note that it peaks around 200 000 K, with drops around 10^5, 10^6 and 10^7 K. *ROSAT* is primarily sensitive to flux in the 0.2–2.4 keV range. The triangles connected by the long-dashed curve are the integrated cooling function after first multiplying by the *ROSAT* response curve. *ROSAT* is insensitive

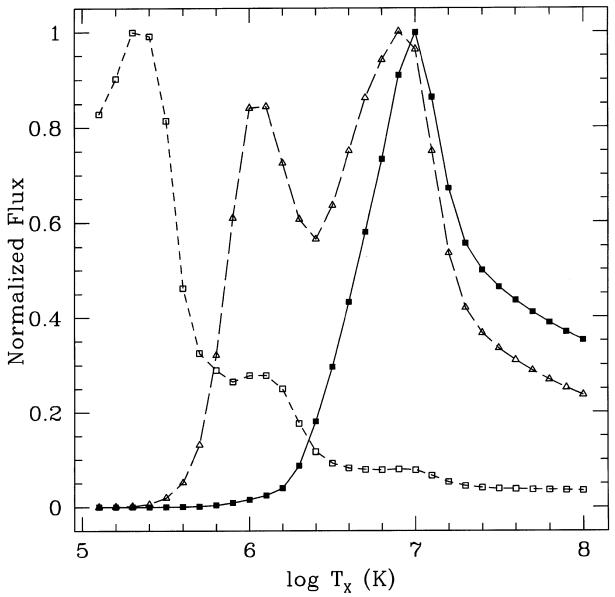

Figure 4. A figure to demonstrate where cooling by lines is maximized. The short-dashed line indicates how the energy integrated cooling function $\Lambda_{\rm tot}$ varies with temperature $T_{\rm X}$ for a single-temperature hot plasma. The long-dashed line includes the effect of the *ROSAT* sensitivity function. Finally, the solid line shows how the cooling varies when both the *ROSAT* sensitivity and wind attenuation are included. In this last case, a single prominent peak occurs around 10^7 K. Note that the points are for individual calculations, and the curves have been individually normalized to their peak values, resulting in a relative *ROSAT* passband flux.

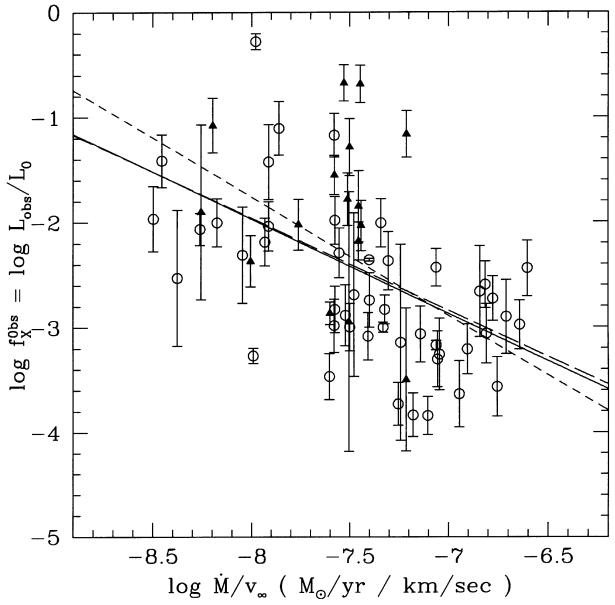

Figure 5. A plot of the filling factor $f_{\rm X}^{\rm obs}$ against the wind density scale $\dot{M}/v_\infty$. Circles are for WN stars, and triangles for WC stars. The errorbars reflect quoted measurement errors. Three linear regressions are shown as discussed in the text. The solid line is taken as our best fit, which is a weighted regression based on measurement errors and an additional but a priori unknown spread relating to variations in abundance and $T_{\rm X}$ among the sample stars. This line has a power-law slope of $m \approx -0.9$ (see Table 6), consistent with the $m \approx -1$ slope derived for O stars. However, the data are indeed quite noisy, so that we can probably only conclude that the sample is not inconsistent with this slope.

to gas below 300 000 K (as noted by Cohen, Cassinelli & MacFarlane 1997), and its sensitivity to hot gas above 20 million degrees drops steadily with $T_{\rm X}$. There exist two distinctive peaks around 1 and 10 million degrees. However, we also know that the WR winds are optically thick to X-rays, with a roughly power-law dependence of the cross-section with energy (see Fig. 1). The final curve with filled boxes connected by a solid line is for the integrated cooling function as first multiplied by the *ROSAT* response and a canonical power law of $E^{-2.5}$ to represent the effects of the energy-dependent wind attenuation. A well-defined peak around 10 million degrees results. This temperature corresponds to maximal cooling appropriate for isothermal shocks, in contrast to the radiative shocks considered by Feldmeier et al. (1997). The exact wind attenuation dependence on E will vary from star to star, as well as the exact cooling curve, so that the filling factors which we derive below are not *true* minima in any absolute sense, but rather minimized within the assumptions that we have adopted.

Choosing $T_{\rm X} = 10^7$ K as fixed for the hot gas component in *all* WR winds, we have recomputed the filling factors and plotted them against those expected from the Kudritzki et al. (1996) relation in Fig. 3(b). As an ensemble, the filling factors have dropped by about 1 dex as compared to Fig. 3(a) of the previous section, but they still lie systematically about 1 dex above the O-star filling factors. Note, however, that the WN sample does loosely follow a linear relation with the Kudritzki et al. relation, implying that the filling factors probably scale roughly as the inverse of $\dot{M}/v_\infty$, but shifted up by an order of magnitude from the O stars.

3.4 Dependence of filling factors on $\dot{M}/v_\infty$

Having derived filling factors, we now want to test empirically whether the filling factors scale like $(\dot{M}/v_\infty)^{-1}$ as assumed or not. In Fig. 5 we explicitly show the minimized filling factors as plotted against $\dot{M}/v_\infty$. The expectation is that the points should fall along a straight line of slope ≈ -1 in this log–log plot. The data are terribly noisy, so we have computed several weighted linear regressions, using the same methods as for comparing $L_{\rm X}$ to L_* and $\dot{M}/v_\infty$. The results of the line fitting is summarized at the bottom of Table 6. Three lines are plotted in Fig. 5 for fits to the entire ensemble of points (WN and WC together), including WR 25. The first line is shown as short-dashed. In this case, weights $w_{\rm i} = 1/\sigma_{\rm i}^2$ based on measurement errors only were used. The line has a slope $m \approx -1.1$, somewhat steeper than desired. In fact, it is the rather large filling factor of WR 25, owing to unusually high $L_{\rm X}$, combined with its small standard deviation, that is affecting this slope.

Two more fits were evaluated, this time with weights $w_{\rm i} = 1/(\sigma_{\rm i}^2 + \sigma_0^2)$, where σ_0 represents an additional dispersion in the data owing to variations in abundances and hot gas temperatures from what has been assumed in the model, as was previously discussed. The two lines are for $\sigma_0 = 0.69$ and 35. The two lines are almost indistinguishable. Since $\sigma_0 = 0.69$ is already about twice the typical measurement error, the weights for many points are dominated by σ_0, which tends to give equal significance to these points. Therefore it is not surprising that the two lines are so similar. The slope is $m \approx -0.9$, quite close to the expected value of -1, especially given the substantial dispersion in the data. A conservative conclusion is that the data are not inconsistent with the empirical relation $f_{\rm X} \propto (\dot{M}/v_\infty)^{-1}$ as observed for O stars.

4 DISCUSSION AND CONCLUSIONS

The X-ray properties of *single* WR stars are in our opinion poorly studied both observationally and theoretically. Colliding wind binaries involving a WR star have naturally received more attention by virtue of being much brighter X-ray sources. Moreover, these systems are expected to show cyclic variations of X-ray emission with orbital phase that might straightforwardly be used to test theoretical models. Single WR stars present a greater challenge to observers, since they tend to be fainter sources and the production of the X-ray emission is less well-understood. The data set for single WR stars consists largely of low S/N broad-band all-sky survey results from RASS, although some pointed observations of higher S/N do exist. Observations also exist from *Einstein* and other missions, but the number of single stars detected is smaller.

Using the RASS sample, a plot of L_X versus L_{Bol} for single WN and WC stars does indeed appear to be lacking correlation, as first pointed out by Wessolowski (1996). Compared to Paper I, we have rescaled the X-ray luminosities of Pollock et al. (1995) to the assumed distances from Koesterke & Hamann (1995) and Hamann & Koesterke (1998), to be consistent with wind parameters (e.g., $\dot{M}$) that we take from those papers. We note that due to the rescaling and the addition of sources that do not have wind parameters from the optical analysis but do have L_X values from Pollock et al., we have recomputed weighted mean X-ray luminosities for the WN and WC subclass in the *ROSAT* band 0.2–2.4 keV. The values are $L_X = 4.3 \pm 0.7 \times 10^{32}\,\mathrm{erg\,s^{-1}}$ for WN types and $L_X = 1.5 \pm 0.5 \times 10^{32}\,\mathrm{erg\,s^{-1}}$ for WC stars. These are only slightly larger (≈5 per cent) than the values quoted in Paper I. There may be some hint that L_X for WN and WC stars increases with the ratio $\dot{M}/v_\infty$ as roughly the cube root (see Table 6), but it is not especially significant.

Using the RASS sample, we have considered two 'experiments'. In the first we assumed that the empirical relations derived by Kudritzki et al. (1996) from *ROSAT* observations of O stars could be applied to WR stars. These relations predict typical hot gas temperatures of around 10^8 K and filling factors of about 10^{-4}. These values are not mutually consistent with the *ROSAT* data. If the temperature of the gas is truly around 10^8 K, then our exospheric models demand filling factors about 2 dex larger than predicted.

The second experiment consisted of maximizing the cooling function (i.e., under the assumption of isothermal shocks), modulo the expected wind attenuation and the *ROSAT* response function, to derive lower limits for the hot gas filling factor. A rough analysis revealed that for a given filling factor, the X-ray emissivity is maximized for $T_X \approx 10^7$ K. Using this value for *every* WR star, the filling factors required to match the observations dropped by a full order of magnitude, yet remained larger than those predicted with the O-star relation by about 1 dex. Although the results of this second experiment seem more in line

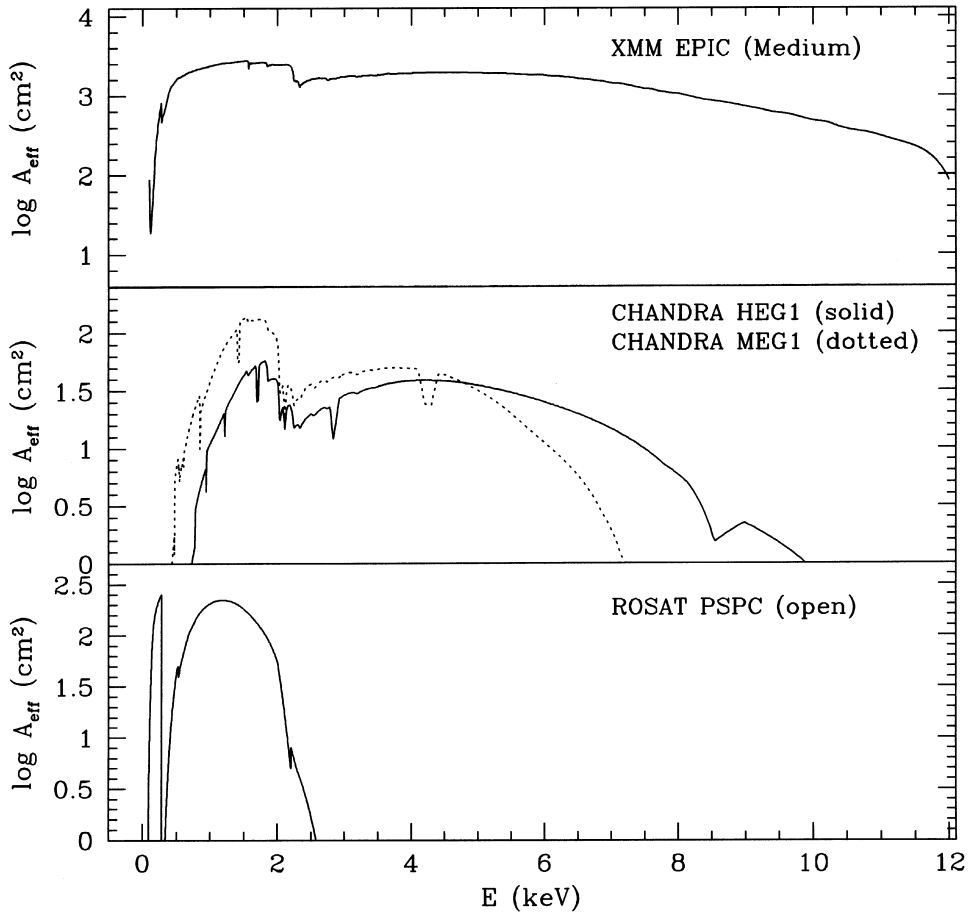

Figure 6. A comparison of instrumental sensitivities in terms of effective area against energy for *XMM*-EPIC (top; *XMM* Dahlem & Schartel 1999), *Chandra* HEG and MEG (middle; credit CXC/SAO), and *ROSAT* PSPC (bottom; Zimmermann et al. 1998; ESAS User's Guide http://wave.xray.mpe.de/exsas/users-guide). The latest instruments have much superior collecting area, sensitivity to high X-ray energies, and spectral resolution (not shown).

with our expectations (i.e., somewhat more similar to the O-star results), we qualify our interpretation by noting that spectral data are truly needed to better constrain the X-ray temperatures and filling factors.

Finally, we considered linear regressions for the filling factor f_X versus the ratio $\dot{M}/v_\infty$. We find that the data appear to be broadly consistent with the assumption of $f_X \sim (\dot{M}/v_\infty)^{-1}$, which is also found empirically for O stars. This seems to hold for WN stars alone, or for WN and WC stars combined. It does not hold for the WC stars alone, but they constitute a much smaller sample, so that the combination of relatively few points with large errors leads to a largely indeterminate fit. It is probably fair to say that f_X seems to decrease with $\dot{M}/v_\infty$ and is not inconsistent with a power-law index of -1.

Is this result simply an artefact of our model? We assume the X-ray luminosity is of the form $L_X = L_0 f_X$, with $L_0 \propto \dot{M}/v_\infty$ for optically thick winds, and we derive filling factors from data via $f_X^{obs} = L_X^{obs}/L_0$. Only if L_X^{obs} is essentially insensitive to $\dot{M}/v_\infty$ will f_X^{obs} vary inversely with $\dot{M}/v_\infty$. Clearly, if the observed X-ray luminosity had varied, say, linearly with $\dot{M}/v_\infty$, then we should have found a flat distribution for f_X^{obs}, and we could have rejected the hypothesis of Paper I that $f_X \propto (\dot{M}/v_\infty)^{-1}$. We concede that our conclusion on this point is model-dependent (e.g., Owocki & Cohen 1999 use a slightly different prescription), and that there might possibly be a roughly cube-root dependence of L_X with $\dot{M}/v_\infty$, but we find that, at the quality of the data, our model appears to be self-consistent.

A new era is upon us with the successful operation of *Chandra* and the launch of *XMM*, both X-ray satellites having much larger collecting areas and substantially better spatial and spectral resolutions than previous missions (see Fig. 6). Motivated by these advances, the purpose of this paper has been to interpret the existing broad-band data for the X-ray emission from WR stars as obtained by *ROSAT*. We have modelled the X-ray emission using an exospheric approach that includes approximations to account for the effect of non-solar abundances for the cooling due to lines and for the wind attenuation. Using this model, we have sought to constrain the temperature T_X of the hot gas and its filling factor f_X. The results presented here suggest that the X-ray emission from WR stars holds great promise for aiding our understanding of these unusual and extreme stellar winds. It is evident that the existing data set is badly lacking in quality, and a push to obtain even just the basic X-ray spectral shape from single WR stars would be a significant step forward.

ACKNOWLEDGMENTS

We express appreciation to J. C. Brown and D. Cohen for helpful discussions on this topic, and especially to D. A. MacDonald for his input at the early stages of this work. The referee, A. Feldmeier, is also gratefully acknowledged for remarks leading to improvements in the paper. This research was supported by a PPARC grant (RI, LMO), an RS/NATO Fellowship (LMO), and an undergraduate summer student grant from the Department of Physics and Astronomy at the University of Glasgow (CF).

REFERENCES

Balucińska-Church M., McCammon D., 1992, ApJ, 400, 699
Baum E., Hamann W.-R., Koesterke L., Wessolowski U., 1992, A&A, 266, 402
Castor J. I., Abbott D. C., Klein R. I., 1975, ApJ, 195, 157 (CAK)
Cohen D. H., Cassinelli J. P., MacFarlane J. J., 1997, ApJ, 487, 867
Dahlem M., Schartel N., eds, 1999, XMM User's Handbook, Issue 1.1, XMM–PS–GM–14
dos Santos L. C., Jatenco-Pereira V., Opher R., 1993, ApJ, 410, 732
Feldmeier A., Kudritzki R.-P., Palsa R., Pauldrach A. W. A., Puls J., 1997, A&A, 320, 899
Gayley K. G., Owocki S. P., 1995, ApJ, 446, 801
Gayley K. G., Owocki S. P., Cranmer S. R., 1995, ApJ, 442, 296
Hamann W.-R., Koesterke L., 1998, A&A, 333, 251
Hillier D. J., Kudritzki R. P., Pauldrach A. W., Baade D., Cassinelli J. P., Puls J., Schmitt J. H. M. M., 1993, A&A, 276, 117
Ignace R., Oskinova L. M., 1999, A&A, 348, L45 (Paper I)
Ignace R., Cassinelli J. P., Bjorkman J. E., 1996, ApJ, 459, 671
Kato M., Iben I., 1992, ApJ, 394, 305
Koesterke L., Hamann W.-R., 1995, A&A, 299, 503
Koyama K., Maeda Y., Tsuru T., Nagase F., Skinner S., 1994, PASJ, 46, L93
Kudritzki R. P., Palsa R., Feldmeier A., Puls J., Pauldrach A. W. A., 1996, in Zimmerman H. U., Trümper J., Yorke H., eds, Röntgenstrahlung from the Universe. MPE Report 263, p. 9
Lucy L. B., Abbott D. C., 1993, ApJ, 412, 771
Maeda Y., Koyama K., Yokogawa J., Skinner S., 1999, ApJ, 510, 967
Nugis T., Crowther P. A., Willis A. J., 1998, A&A, 333, 956
Owocki S. P., Cohen D. H., 1999, ApJ, 520, 833
Poe C. H., Friend D. B., Cassinelli J. P., 1989, ApJ, 337, 888
Pollock A. M. T., 1987, ApJ, 320, 283
Pollock A. M. T., Haberl F., Corcoran M. F., 1995, in van der Hucht K. A., Williams P. M., eds, Proc. IAU Symp. 163, Wolf–Rayet Stars: Binaries, Colliding Winds, Evolution. Kluwer, Dordrecht, p. 191
Raymond J. C., Smith B. W., 1977, ApJS, 35, 419 (RS)
Seward F. D., Chlebowski T., 1982, ApJ, 256, 530
Skinner S. L., Itoh M., Nagase F., 1997, New Astronomy, 3, 37
Springmann U., 1994, A&A, 289, 505
Stevens I. R., Corcoran M. F., Willis A. J., Skinner S. L., Pollock A. M. T., Nagase F., Koyama K., 1996, MNRAS, 283, 589
van der Hucht K. A., Cassinelli J. P., Williams P. M., 1986, A&A, 168, 111
Verner D. A., Yakovlev D. G., 1995, A&AS, 109, 125
Wessolowski U., 1996, in Zimmerman H. U., Trümper J., Yorke H., eds, Röntgenstrahlung from the Universe. MPE Report 263, p. 75
Wessolowski U., Hamann W.-R., Koesterke L., Hillier D. J., Puls J., 1995, in van der Hucht K. A., Williams P. M., eds, Proc. IAU Symp. 163, Wolf–Rayet Stars: Binaries, Colliding Winds, Evolution. Kluwer, Dordrecht, p. 174
White R. L., Long K. S., 1986, ApJ, 310, 832
Willis A. J., 1991, in van der Hucht K. A., Hidayat B., eds, Proc. IAU Symp. 143, Wolf–Rayet Stars and Interrelations with Other Massive Stars in Galaxies. Kluwer, Dordrecht, p. 265
Woan G., 2000, The Cambridge Handbook of Physics Formulas. Cambridge Univ. Press, Cambridge
Wolf C. J. E., Rayet G. A. P., 1867, Comptes Rendus, 65, 291
XMM Users' Handbook, Issue 1.1, Dahlem M., Schartel N. eds, 1999, XMM-PS-GM-14,
Zimmermann U., Boese G., Becker W., Belloni T., Döbereiner S., Kahabka P., Schwentker O., 1998, EXSAS User's Guide

APPENDIX A: COOLING FUNCTION FOR WOLF–RAYET ABUNDANCES

For the case when lines dominate the X-ray emission spectrum, the Raymond–Smith cooling function can be approximated in the compact form

$$\Lambda_{RS}(E) \approx \sum_k \left(\frac{n_k}{n_H}\right)_\odot P_k(E), \tag{A1}$$

where n_k is the number density for the appropriate species, ion,

and level corresponding to the factor $P_{\rm k}$ representing the various emission processes contributing to the cooling function at energy E. Correspondingly, the emissivity is then

$$j_\nu(E) = \frac{1}{4\pi} n_{\rm e} n_{\rm H} \Lambda_{\rm RS}. \tag{A2}$$

However, this parametrization of the cooling function is difficult to use for Wolf–Rayet winds where the hydrogen number density approaches zero. Moreover, the Wolf–Rayet abundances are far from solar. We therefore derive here a simplistic modification to the classical Raymond–Smith cooling function for Wolf–Rayet winds.

We begin by defining our emissivity as

$$j_\nu(E) = \frac{1}{4\pi} n_{\rm e} n_{\rm i} \Lambda_\nu, \tag{A3}$$

with

$$\Lambda_\nu = \sum_k \left(\frac{n_{\rm k}}{n_{\rm i}}\right) P_{\rm k}(E). \tag{A4}$$

Thus the problem reduces to relating Λ_ν to $\Lambda_{\rm RS}$. This is done as follows:

$$\Lambda_\nu = \sum_k \left(\frac{n_{\rm k}}{n_{\rm i}}\right) \left(\frac{n_{\rm H}}{n_{\rm k}}\right)_\odot \left(\frac{n_{\rm k}}{n_{\rm H}}\right)_\odot P_{\rm k}(E) \tag{A5}$$

$$= \left(\frac{n_{\rm H,\odot}}{n_{\rm i}}\right) \sum_k \left(\frac{n_{\rm k}}{n_{\rm k,\odot}}\right) \left(\frac{n_{\rm k}}{n_{\rm H}}\right)_\odot P_{\rm k}(E). \tag{A6}$$

The ion number density and ionized hydrogen number density can be extracted from the summation. Since they are both proportional to mass density, their ratio becomes $n_{\rm H,\odot}/n_{\rm i} = \mu_{\rm i}/\mu_{\odot,{\rm H}}$. Further, we define the parameter $\tilde{A} = (n_{\rm k})/(n_{\rm k})_\odot$. If this parameter is constant for every k, it too can be removed from the summation. (Alternatively, $\tilde{A}$ could represent an appropriate ensemble mean when the cooling function is sampled over a broad energy bandpass, as is the case for *ROSAT*.) Making these substitutions, the expression becomes

$$\Lambda_\nu = \frac{\mu_{\rm i}}{\mu_{\odot,{\rm H}}} \tilde{A} \Lambda_{\rm RS}. \tag{A7}$$

APPENDIX B: LINEAR REGRESSION ANALYSIS OF THE *ROSAT* DATA AND MODEL RESULTS

Here we briefly review the method of weighted linear regression used in our analysis. The method is fairly standard. We adopt the notation of Woan (2000).

For data consisting of N points $\{x_{\rm i}\}$ and $\{y_{\rm i}\}$, we define a set of weights $\{w_{\rm i}\}$ with

$$w_{\rm i} = \frac{1}{\sigma_{\rm i}^2 + \sigma_0^2}. \tag{B1}$$

The standard deviations $\{\sigma_{\rm i}\}$ are measurement errors for the values $\{y_{\rm i}\}$, whereas σ_0 is some other intrinsic spread to the data, either known or unknown and possibly zero.

The data are assumed to be linear as $y = mx + b$. We make the following convenient definitions:

$$d_{\rm i} = y_{\rm i} - m x_{\rm i} - b, \tag{B2}$$

$$W = \sum w_{\rm i}, \tag{B3}$$

$$(\bar{x}, \bar{y}) = \frac{1}{W}\left(\sum w_{\rm i} x_{\rm i}, \sum w_{\rm i} y_{\rm i}\right), \tag{B4}$$

$$D = \sum w_{\rm i} (x_{\rm i} - \bar{x})^2. \tag{B5}$$

With these definitions, the slope and intercept of the best-fitting line to the data are

$$m = \frac{1}{D} \sum w_{\rm i} (x_{\rm i} - \bar{x}) y_{\rm i}, \tag{B6}$$

$${\rm var}[m] = \frac{1}{D} \frac{\sum w_{\rm i} d_{\rm i}^2}{N-2}, \tag{B7}$$

$$b = \bar{y} - m\bar{x}, \tag{B8}$$

$${\rm var}[b] = \left(\frac{1}{W} - \frac{\bar{x}}{D}\right) \frac{\sum w_{\rm i} d_{\rm i}^2}{N-2}. \tag{B9}$$

The goodness of fit is determined by the reduced chi-square χ_ν^2, where ν is the number of degrees of freedom ($N - 2$ in this case). The goodness of fit is given by

$$\chi_\nu^2 = \frac{\sum w_{\rm i} d_{\rm i}^2}{N-2}. \tag{B10}$$

For $\sigma_0 = 0$, the dispersion in the data is assumed to arise solely from measurement errors. For $\sigma_0 \gg \sigma_{\rm i}$ for all i, the dispersion of the data is essentially unrelated to measurement errors. Note that in this case, (a) $w_{\rm i}$ is approximately constant for all i, so that each point is treated as having equal weight in the regression, and (b) the value of χ_ν^2 is driven toward zero, since the weights are essentially all quite small (i.e., increasing values of σ_0 naturally lead to an ever better fit to the data). If σ_0 is a priori unknown, its most likely value is found by requiring $\chi_\nu^2 = 1$.

This paper has been typeset from a TEX/LATEX file prepared by the author.